MICROBIAL DRUG RESISTANCE
Volume 8, Number 4, 2002

Cellular Location and Function of the P-Glycoproteins (EhPgps) in *Entamoeba histolytica* Multidrug-Resistant Trophozoites

CECILIA BAÑUELOS,[1] ESTHER OROZCO,[1] CONSUELO GÓMEZ,[2] ARTURO GONZÁLEZ,[1] OLIVIA MEDEL,[2] LEOBARDO MENDOZA,[1,2] and D. GUILLERMO PÉREZ[2]

ABSTRACT

We have studied the cellular location and the efflux pump function of the *Entamoeba histolytica* P-glycoproteins (EhPgps) in drug-sensitive and -resistant trophozoites. Polyclonal antibodies against the EhPgp384 polypeptide (375–759 amino acids) revealed a 147-kDa protein by Western blot. The band intensity correlated with the emetine-resistance of the trophozoites. Through the confocal microscope, using the anti-EhPgp384 and fluorescein secondary antibodies, the EhPgps were found in a complex vesicular network, in the plasma membrane and outside of the cells. Transmission electron microscopy assays confirmed that drug-resistant trophozoites presented four to five times more EhPgps than sensitive cells. Fluorescence co-localization experiments using rhodamine-123 (R123) and the anti-EhPgp384 antibodies suggested the interaction between EhPgps and the drug. R123 efflux kinetics evidenced that the emetine-resistant trophozoites displayed a drug efflux kinetic four times higher than the drug-sensitive trophozoites, which was reduced by verapamil in both cases. EhPgps may participate in avoiding drug accumulation in the trophozoites by two putative mechanisms: (1) the direct extrusion of the drug from the plasma membrane, and (2) an indirect transport mechanism in which the drug is trapped by EhPgps and concentrated within vesicles that drive the drug to the plasma membrane.

INTRODUCTION

ENTAMOEBA HISTOLYTICA, the protozoan responsible for human amoebiasis, infects 10% of the world's population, causing 50 million cases of dysentery or liver abscesses and killing 100,000 persons per year around the world.[45] Due to the difficulties in changing the sanitary conditions and eliminating the infection spread, amoebiasis is primarily controlled by drug treatment of symptomatic individuals.[28]

Drug resistance has emerged as an impediment in the treatment and control of many infectious diseases, including those produced by protozoa. *E. histolytica* strains present different drug susceptibilities,[7,17,37] and there are also case reports of failed drug treatments.[4,5,22] In addition, drug-resistant lines have been generated in the laboratory,[29,34] suggesting that *E. histolytica* may naturally develop drug resistance. These data make the study of the mechanisms involved in the development of drug resistance in this parasite of the highest priority.

The overexpression of a surface P-glycoprotein (Pgp) produces the multidrug resistance (MDR) phenotype in mammalian tumor cells[26] and in protozoan parasites,[42] including *Plasmodium,*[8] *Trichomonas,*[24] *Giardia,*[43] *Leishmania,*[32] and *Entamoeba*.[3] Pgps are energy-dependent drug efflux pumps that act as transporters in MDR cells, maintaining the intracellular drug concentration below cytotoxic levels.[16] Pgps have also been involved in removing xenobiotic agents from the cells, in metabolism and translocation of lipids, in apoptosis, in cytokines transport, and as ion channels or regulators of cell swelling-activated chloride channels.[10,25]

Emetine-resistant mutants of *E. histolytica* (clone C2) present cross resistance to colchicine, diloxanide, and iodoquinol.[29,30] The drugs are poorly accumulated in the tropho-

[1]Department of Experimental Pathology, CINVESTAV-IPN. A. P. 14-740, México 07300, D.F.
[2]Program of Molecular Biomedicine, ENMyH-IPN, Fracc. "La Escalera," Ticomán, CP 07320, México, D.F.

zoites and, as in mammalian cells, drug resistance is reversed by calcium channel blockers.[3] Drug-resistant trophozoites overexpress a 4-kb *mdr*-like transcript[36] and they have at least four *EhPgp* genes (*EhPgp1, EhPgp2, EhPgp5,* and *EhPgp6*).[11,12] The *EhPgp1* and *EhPgp5* genes are overexpressed in the emetine-resistant clone C2, and their expression is regulated at transcriptional level.[19,33] The *EhPgp5* gene is transcribed only in the presence of a high drug concentration and after the *EhPgp1* gene is overexpressed.[30]

Although we know that in *Xenopus laevis* oocytes, the EhPgp5 protein functions as a Cl^- current inductor,[10] the functions performed by the EhPgps in the trophozoites have not been elucidated. Here, we generated antibodies against an EhPgp recombinant polypeptide to study the location of the EhPgps in trophozoites with different drug sensitivities. Moreover, taking advantage of the physical–chemical properties of the cationic dye rhodamine-123 (R123),[6] we performed dual-fluorescence experiments to determine the physical relationship of EhPgps and R123 inside the cells and to investigate how this drug is expelled from trophozoites. Our data showed that EhPgps are located in vesicles that seem to concentrate and drive the drug to the plasma membrane, to expel it out of the cells.

MATERIALS AND METHODS

Culture of E. histolytica *trophozoites*

Trophozoites of *E. histolytica* clones A and C2 (strain HM1:IMSS)[29] were axenically cultured in TYI-S-33 medium.[14] The clone C2(225) was cultured in the presence of 225 μM emetine. Transfected trophozoites (clones Aneo and AneoPgp5) were grown in the presence of 10 μg/ml of G418. All clones were harvested during exponential growth phase as described.[14]

Transfection assays

Transfection of *E. histolytica* trophozoites was carried out by the electroporation method with 100 μg of pEhNEO or pEhNEOPgp5 plasmids, as previously described.[21] Electroporated trophozoites were transferred into plastic flasks (Nunc) containing 30 ml of TYI-S-33 medium and then, incubated at 37°C for 48 hr in the presence of 100 μg/ml of G418.

Identification of the EhPgps antigenic regions by computational analysis

To find the most antigenic regions of EhPgps, we used hydropathy plots and the DNAStar program.[15] Oligonucleotides design was performed with the aid of the Oligo program.[15]

Amplification and cloning of the 1,152-bp EhPgp*-encoding fragment*

Amplification of the 1,152-bp fragment of the *EhPgp1* gene, corresponding from 375 to 759 amino acids (EhPgp384) was performed using the sense 5′-CTGGAATTCAAATCCCAGATATTGATT-3′ and the antisense 5′-AGCAAGCTTCCTGTTAGCTTGTTCATC-3′ oligonucleotides, 100 ng of total *E. histolytica* DNA as template and 2.5 U of *Taq* DNA polymerase (Gibco) for 30 cycles (94°C for 30 sec, 48°C for 35 sec, and 72°C for 2 min), according to standard methods.[2] The PCR product was cloned in frame into the *Eco*RI and *Hin*dIII restriction sites of the pRSETA expression vector (Invitrogen), generating the pRSETA-*Pgp1152* plasmid. The orientation and sequence of the construction were confirmed by DNA sequencing, using the method described by Sanger.[39]

Expression and purification of the EhPgp384 recombinant polypeptide

BL21(DE3) bacteria were transformed with the pRSETA-*Pgp1152* plasmid and grown with 1 mM isopropyl-β-D-thiogalactopyranoside (IPTG) at 37°C for 3 hr. Bacterial proteins were separated by 10% SDS-PAGE and detected by Coomassie blue staining. The EhPgp384 recombinant polypeptide was partially purified under denaturing conditions by metal affinity chromatography using a nickel-chelating resin (Ni^{2+}-NTA agarose, Qiagen). Further purification was obtained after electroelution of the protein from 10% SDS-PAGE.[2]

Generation of antibodies against the EhPgp384 recombinant polypeptide

New Zealand rabbits were subcutaneously immunized with 100 μg of the purified EhPgp384 polypeptide, emulsified in Freund's complete adjuvant.[2] Booster immunizations were performed every 14 days during four times with the same amount of the recombinant protein, using Freund's incomplete adjuvant. Seven days after the last inoculation, the immune serum was obtained, tested, and titered.

Detection of EhPgps *mRNAs by the reverse transcriptase-polymerase chain reaction (RT-PCR)*

Poly(A)$^+$ RNA from trophozoites was obtained using an oligo-dT oligomer coupled to polystyrene-latex particles (Qiagen). cDNA was synthesized using 1 μg of DNase-treated mRNA, 10 mM dNTPs, 200 U AMV reverse transcriptase (Gibco), and 100 ng each ASPgp1 (5′-CTGCTAATATACATAAC-3′), ASPgp5 (5′-GTCAAACAAGAAATAGGATGG-3′), and ASNEO (5′-TTAGAAGAACTCGTC-3′) oligonucleotides, for *EhPgp1, EhPgp5,* and *NEO*-specific sequences, respectively, at 42°C for 1 hr. PCR amplification was carried out with 5 μl of the cDNA mixture, 1 U of amplitaq polymerase, and 2 mM dNTPs. Each PCR cycle comprised 45 sec at 94°C, 30 sec at 49°C, and 50 sec at 72°C. *EhPgp1* and *EhPgp5* gene-specific sequences were amplified using 100 ng of ASPgp1 and SPgp1 (5′-GGTTATGGCAGCAGG-3′) or ASPgp5 and SPgp5 (5′-GTAGGAGGTGCAGTATTCCC-3′) primers, yielding fragments of 300 and 270 bp, respectively. As an internal control, the AS-NEO and SNEO (5′-ATGATTGAACAAGATGG-3′) primers were used to amplify a 700-bp band of the *NEO* gene. PCR was carried out in a Perkin-Elmer thermal cycler for 29 cycles, and products were visualized on 12% polyacrylamide gels.

Western blot assays

Ten and 50 μg of total extracts from bacteria and trophozoites, respectively, were analyzed by 10% SDS-PAGE and transferred to nitrocellulose membranes. Western blot assays[2] were carried out using the anti-EhPgp384 antibodies at 1:2,000

and 1:25 dilutions for bacterial and trophozoite extracts, respectively. Membranes were then incubated with horseradish peroxidase (HRP)-conjugated goat anti-rabbit immunoglobulin G (IgGs) (Zymed) at 1:30,000 and 1:1,000 dilutions for bacterial and trophozoite extracts, respectively. Antigen–antibody reactions were revealed using a fresh preparation of 3 mg/ml of 4-chloro-1-naphthol until the color was developed. Membranes were also treated with monoclonal mouse anti-actin antibodies (kindly given by Dr. Manuel Hernández, CINVESTAV, México) and HRP-conjugated anti-mouse IgGs at 1:1,000 and 1:2,000 dilutions, respectively, and revealed with 4-chloro-1-naphthol.

Laser confocal microscopy assays

Trophozoites growing at logarithmic phase were harvested, washed twice in phosphate-buffered saline (PBS) pH 7.4, fixed with 4% paraformaldehyde at 37°C for 60 min, and permeabilized with 1% Triton X-100 for 30 min. Then, trophozoites were incubated with 1% bovine serum albumin (BSA) for 20 min at room temperature (RT), washed twice with PBS-1% Triton, and incubated overnight at 4°C with the anti-EhPgp384 antibodies (1:100) or with the preimmune serum or PBS. Trophozoites were washed twice with PBS-1% Triton, incubated with fluorescein (FITC)- or rhodamine (TRITC)-labeled goat anti-rabbit IgGs (Zymed) for 90 min at 37°C and washed with PBS-1% Triton. Finally, cells were incubated with 1 mg/ml of propidium iodide for 5 min and observed through an inverted microscope (Nikon) attached to a laser confocal system (MRC-1024, BioRad).

For the R123 cellular distribution assay, trophozoites were incubated with 5 μg/ml of R123 for 30 min at 37°C, washed twice in cold PBS, resuspended in R123-free medium, and processed for immunofluorescence as described above.

Transmission electron microscopy assays (TEM)

For cellular location of the EhPgps by immuno-cryoultramicrotomy,[23] trophozoites were fixed with 4% paraformaldehyde and 0.5% glutaraldehyde in PBS for 1 hr at RT and infused with 2.3 M sucrose containing 25% polyvinylpyrrolidone, average MW 10 000 (Sigma), in PBS with 0.12% glycine for 45–60 min at RT. Samples were placed on standard Reichert-Jung aluminum pins and immersed in liquid nitrogen at −80°C. Grids were placed section-down for 3 min each on three puddles of 0.12% glycine-PBS to block the paraformadehyde and wash out sucrose. Then, sections were blocked with 10% fetal bovine serum (FBS) for 30 min at RT and incubated with the anti-EhPgp384 antibodies at 1:30 dilution at 4°C overnight. Grids were washed on three puddles of 0.12% glycine-PBS, 5 min each, placed for 1 hr on 15-nm gold particle-labeled goat anti-rabbit IgGs (Zymed), and profusely washed for 30 min on puddles of distilled water. Then, grids were floated on a drop of 2% methylcellulose (25 centipoise) containing 0.3% uranyl acetate for 10 min on ice.

Efflux kinetics of R123

A total of 10^6 trophozoites of clones A and C2(225) were incubated with R123 (1 μg/ml) for 30 min at 37°C. Then, cells were washed twice with cold PBS and resuspended in R123-free medium without serum. At 0, 1.5, 3, and 4.5 hr, fluorescence in the medium was measured spectrofluorometrically at excitation and emission settings of 515 and 537 nm, respectively, in a LS-50B spectrofluorometer (Perkin Elmer). The R123 concentration was determined by interpolation of the relative fluorescence obtained at each period of efflux time in a R123 standard concentration curve from 0 to 0.1 μg of R123/ml in TYI-S-33 medium without serum. R123 concentration in-

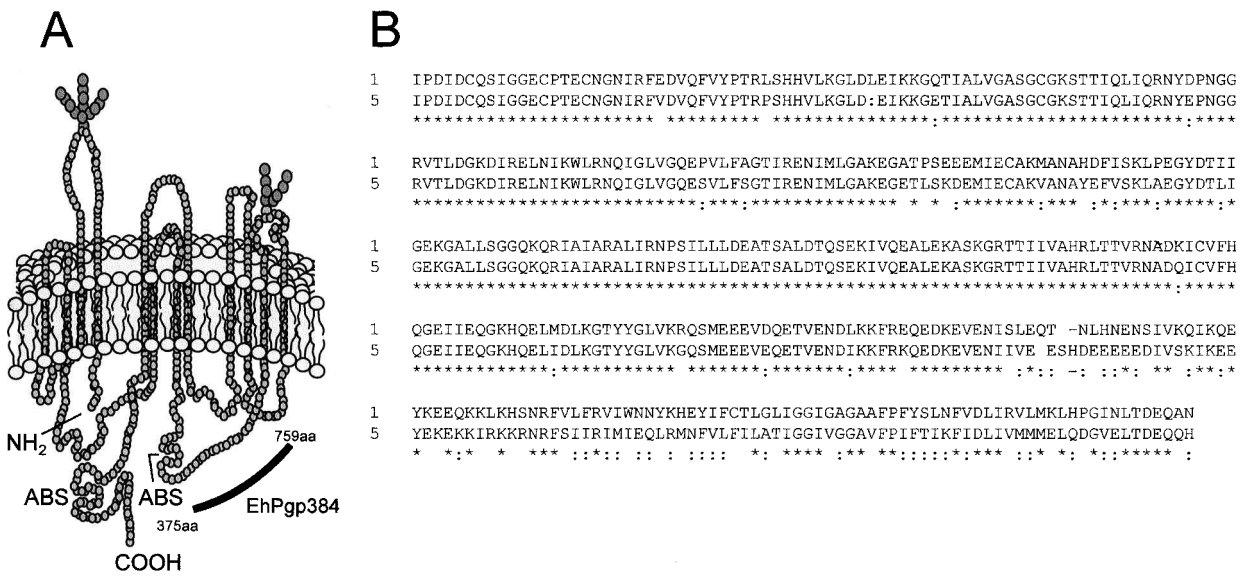

FIG. 1. (**A**) Location of the most antigenic region (residues 375–759, EhPgp384) in a schematic representation of the *E. histolytica* P-glycoproteins (EhPgps). (Black bar) EhPgp384; (branched balls in the extracellular space) putative glycosylation sites; (ABS) ATP binding sites. (**B**) Alignment of the residues 375–759 from the *EhPgp1* (1) and *EhPgp5* (5) gene products. (*) identical residues; (:) compensatory changes.

creased in the medium with a time course that it is well fit by a linear behavior. Thus, constant rates for R123 efflux were estimated using the equation:

$$m = \frac{R123_c - b}{t} \qquad \text{(Eq. 1)}$$

where m is the rate of R123 efflux, $R123_c$ is the R123 concentration at each point measured (ng/ml), t is the time (min), and b corresponds to the y-axis intersection.

To measure the inhibitory effect of verapamil, R123 efflux kinetics were done as described above, incubating the trophozoites in the presence of 15 μM verapamil.

RESULTS

Identification of a highly antigenic region of the EhPgp1 protein by computational analysis

The most antigenic regions of the predicted EhPgp1 amino acid sequence were detected using the DNAStar antigenic determinants prediction program.[15] The highest hydrophylic sequence was found in the cytoplasmic side of the putative protein, from amino acids 375 to 759 (EhPgp384). This fragment includes the amino-terminal ATP-binding site (Fig. 1A) and it has 79% identity with the EhPgp5 protein corresponding region (Fig. 1B). Therefore, it was expected that polyclonal antibodies against this polypeptide would recognize the EhPgp1 and EhPgp5 proteins.

The 1,152-bp DNA fragment coding for the EhPgp384 polypeptide was PCR amplified and cloned in-frame into the pRSETA plasmid (pRSETA-*Pgp1152*). Bacteria transformed with this plasmid expressed a 48-kDa protein (Fig. 2A, lane 2), 42 kDa correspond to the EhPgp384 polypeptide and 6 kDa to the poly-His tail. EhPgp384 was purified by metal affinity chromatography on a nickel-chelating resin as a homogeneous 48-kDa protein (Fig. 2A, lane 3). This polypeptide was used to generate rabbit polyclonal antibodies that recognized a single 48-kDa band in the induced bacterial extracts and also reacted with the purified EhPgp384 recombinant polypeptide (Fig. 2B, lanes 2 and 3). The anti-EhPgp384 antibodies did not react with the bacteria transformed with the pRSETA plasmid (Fig. 2B,

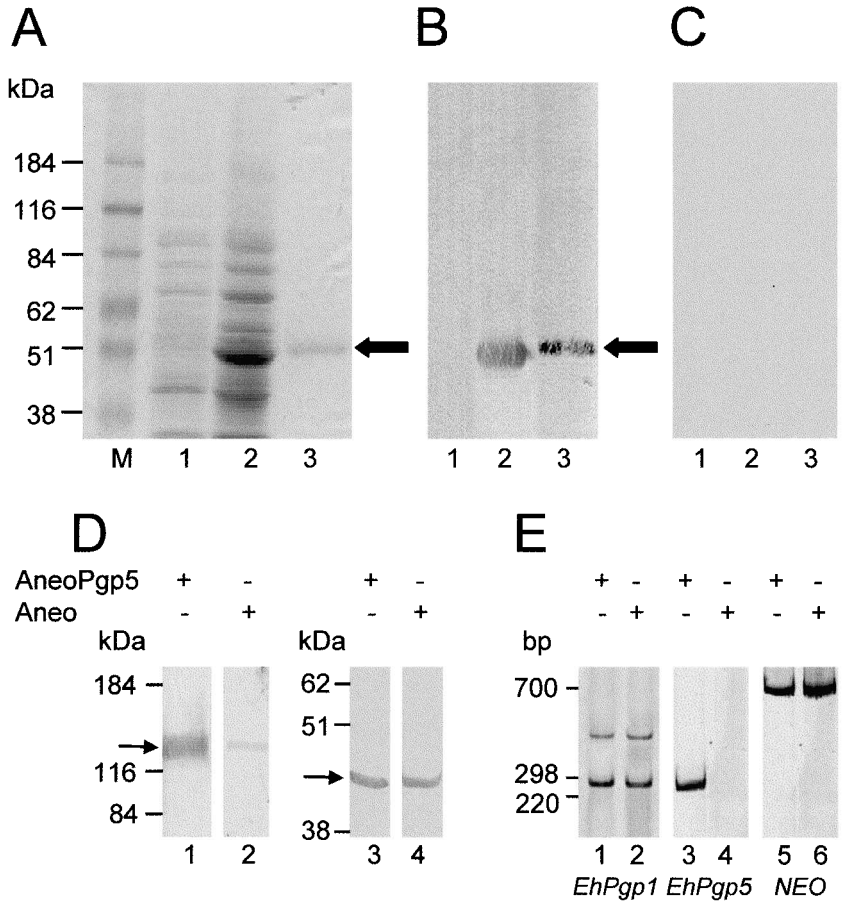

FIG. 2. (**A**) Expression of the EhPgp384 recombinant polypeptide. Molecular weight markers (lane M), protein extracts of BL21(DE3) bacteria transformed with pRSETA vector (lane 1), or with pRSETA-*Pgp1152* plasmid after 3 hr of induction with 1 mM IPTG (lane 2), EhPgp384 Ni^{2+}-affinity-purified recombinant polypeptide (lane 3). (**B**) Immunodetection of the EhPgp384 recombinant polypeptide by the anti-EhPgp384 antibodies and HRP-conjugated goat anti-rabbit IgGs, revealed by 4-chloro-1-naphthol. Lanes 1, 2, and 3 are as in **A**. (**C**) Negative control using preimmune serum. Lanes 1, 2, and 3 were loaded as in **A**. (**D**) Immunodetection of EhPgps and actin expressed by the trophozoites of clone AneoPgp5 (lanes 1 and 3, respectively) or Aneo (lanes 2 and 4, respectively). Membranes were treated as above. (**E**) RT-PCR assays to detect the expression of *EhPgp1, EhPgp5,* and *NEO* genes. Clone AneoPgp5 (lanes 1, 3, and 5) and clone Aneo (lanes 2, 4, and 6) are shown.

lane 1), and neither the preimmune serum recognized the recombinant protein from induced bacteria (Fig. 2C, lanes 2 and 3).

To investigate if the anti-EhPgp384 antibodies also reacted with the *EhPgp5* gene product, we transfected trophozoites of clone A with the *EhPgp5* gene, using the pEhNEOPgp5 plasmid (clone AneoPgp5). Western blot assays revealed a wide 147-kDa band in the trophozoites expressing the *EhPgp5* gene (Fig. 2D, lane 1). The antibodies developed a weaker 147-kDa band in the extracts obtained from the trophozoites transfected with the pEhNEO plasmid (clone Aneo), carrying the *NEO* gene but lacking the *EhPgp5* gene (Fig. 2D, lane 2). The faint band seen in the trophozoites transfected with the pEhNEO plasmid was probably due to the EhPgp1 protein basally produced by the clone A.[19] Antibodies against actin showed that both lanes were loaded with the same amount of protein (Fig. 2D, lanes 3 and 4).

To confirm that the *EhPgp5* gene was expressed by the AneoPgp5 trophozoites, we performed RT-PCR assays using specific primers for the *EhPgp1* and the *EhPgp5* genes.[12] In the trophozoites of clone Aneo, the *EhPgp1* was amplified but no *EhPgp5* transcript was detected (Fig. 2E, lanes 2 and 4). As expected, the trophozoites of clone AneoPgp5, expressed both *EhPgp1* and *EhPgp5* genes (Fig. 2E, lanes 1 and 3). The *NEO* gene probe was used as an internal control and it was similarly amplified in trophozoites transfected with both plasmids (Fig. 2E, lanes 5 and 6). A non-specific band appeared also when we used the *EhPgp1* oligonucleotides (Fig. 2E, lanes 1 and 2).

Detection of a 147-kDa EhPgp in drug-sensitive and -resistant trophozoites

By Western blot experiments, the anti-EhPgp384 antibodies revealed a 147-kDa protein in total extracts of trophozoites of clones A, C2, and C2(225) (Fig. 3A). As expected, the fainter band was found in trophozoites of the drug-sensitive clone A. A higher amount of the protein was observed in the drug-resistant trophozoites of clone C2, whereas the strongest signal was detected in the trophozoites of clone C2(225). As an internal control, the monoclonal anti-actin antibodies revealed that the same amount of total proteins was loaded in the three lanes (Fig. 3B). Thus, the EhPgp proteins expression correlated with the drug-resistance phenotype of the clones, as it was confirmed by the densitometric analysis, which displayed that the trophozoites of clone C2(225) have three times more EhPgps than those of clone A (Fig. 3C).

Location of EhPgps at the plasma membrane and in cytoplasmic vesicles of E. histolytica *trophozoites*

Through confocal immunofluorescence microscopy, using the anti-EhPgp384 antibodies, the trophozoites of clone A presented a very low signal, mainly at the plasma membrane (Fig. 4A), while the amount of fluorescence in the trophozoites of clone C2 was stronger, and it also appeared in the cytoplasm (Fig. 4B). The highest fluorescence intensity was exhibited by the trophozoites of clone C2(225), where the EhPgps appeared as brighter points in membrane protuberances (Fig. 4C, arrows). We also detected some fluorescent spots out of the cells (data not shown), suggesting that the EhPgps could be secreted by the trophozoites. No appreciable staining of the trophozoites was observed when we used the preimmune serum or when the primary antibodies were omitted (Fig. 4D).

The ultrastructural location of the EhPgps, using the anti-EhPgp384 and gold-conjugated secondary antibodies, also showed the presence of EhPgps in the plasma membrane and in cytoplasmic vesicles. Again, the trophozoites of clone A (Fig. 5A) presented few gold particles, which were abundant in the trophozoites of clone C2(225) (Fig. 5B). When we omitted the anti-EhPgp384 antibodies, no gold particles were detected (Fig. 5C). Interestingly, the EhPgps were located in vesicles of different sizes in both clones (Fig. 5A, B), some of them forming

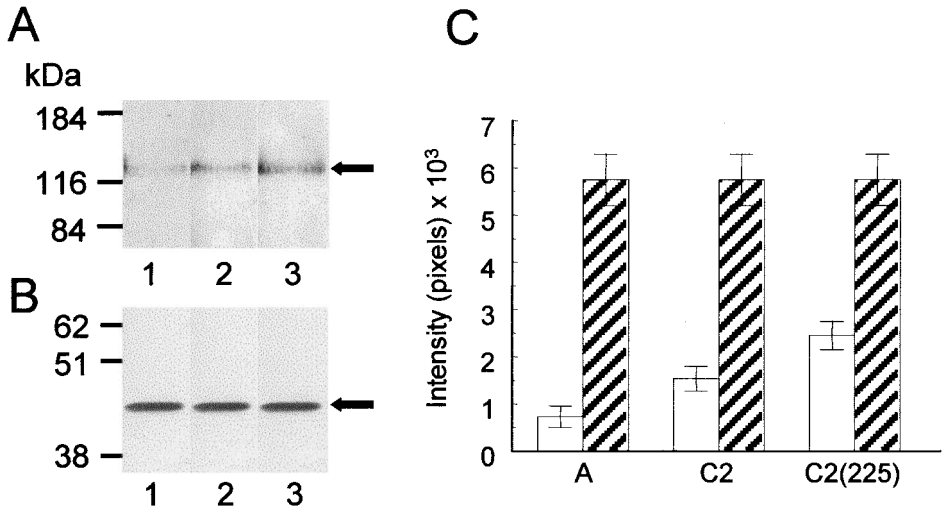

FIG. 3. (**A**) Immunodetection of EhPgp proteins in trophozoites with different drug sensitivities. (**B**) Immunodetection of actin protein as an internal control. Western blot assays were carried out as in Fig. 2B and 2D, except for actin, which was detected by monoclonal antibodies and HRP-conjugated anti-mouse IgGs. Clones A (lane 1), C2 (lane 2), and C2(225) (lane 3). (**C**) Densitometric analysis of A and B (□), EhPgps (■), and actin.

large networks that resemble Golgi-like structures (Fig. 5E, F, G, arrowheads). These images suggested that the EhPgps could be transported through these networks to the plasma membrane (Fig. 5F, G) and probably, to the extracellular space (Fig. 6A, B, arrowheads), because gold particles were found in membrane vesicles and outside the cells.

Gold particles were counted in several randomly selected areas of different pictures of the cells. Trophozoites of clone A presented 15 ± 8 particles/μm^2, whereas those of clone C2(225) showed 54 ± 37 particles/μm^2 inside the cells. In both clones, gold particles were more abundant in the vesicles. Vesicles of trophozoites of clone A showed a mean of 29 ± 12 particles/μm^2, whereas vesicles of trophozoites of clone C2(225) displayed 110 ± 82 particles/μm^2. In the cytoplasm, outside of vesicles, the trophozoites presented also gold particles, but in a lower amount. Trophozoites of clone A showed 3 ± 1 particles/μm^2 and those of clone C2(225) 9 ± 7 particles/μm^2. The amount of gold particles in the extracellular space and at the plasma membrane correlated with the amount of EhPgps detected in the trophozoites, and it was higher in those of clone C2(225) (12 ± 3 particles/μm^2) than in trophozoites of clone A (4 ± 3 particles/μm^2). The high standard deviations obtained from these experiments were due to differences in the amount of gold particles in the vesicles, to the distinct size of the vesicles, and to the sections analyzed. Our TEM results showed that the EhPgps are driven to the plasma membrane by a complex vesicular network system and secreted to the extracellular space.

Association between EhPgps and R123

Next, we investigated the association between EhPgps and the drugs using R123, a fluorescent MDR substrate,[6] and the anti-EhPgp384 antibodies developed by TRITC-conjugated secondary antibodies. For these experiments, we incubated the trophozoites of clone C2(225) for 30 min with 5 μg/ml of R123 to overload the cells with the substrate. Through confocal microscopy, the EhPgps red fluorescence and R123 green fluorescence appeared associated in cytoplasmic vesicles and in several plasma membrane protuberances (Fig. 7A, arrows, and B). R123 in vesicular structures inside the trophozoites suggested that the substrate might be trapped into these vesicles to be expelled outside the cells. Trophozoites, in which we omitted the R123 and the anti-EhPgp384 antibodies, showed no fluorescence (Fig. 7C). The association of the drug with the EhPgps supported the hypothesis that the EhPgps sequester the drug into cytoplasmic vesicles, which are driven to the plasma membrane to be extruded.

Drug efflux in trophozoites of clones A and C2(225)

In previous reports, Ayala *et al.*[3] demonstrated that the trophozoites of clone A and clone C2, resistant to 90 μM emetine [C2(90)], incubated with tritiated emetine for 30 min presented a similar amount of radioactivity in their cytoplasm. At longer times, the trophozoites of clone A kept a higher amount of drug than those of clone C2(90). However, in these experiments, the authors did not study the drug efflux. Thus, it was not possible to determine if the lower radioactivity in the drug-resistant trophozoites after 60, 90, and 270 min of incubation was due to the transport of the drug out of the cells by the EhPgps, or to the fact that the EhPgps did not allow the entrance of more drug to the cells. The microscopy assays carried out here showed the association between EhPgps and R123 inside cytoplasmic vesicles. To test whether the drug was actively extruded, we determined the R123 efflux in trophozoites of clones A and C2(225) preloaded with R123 for 30 min and resuspended in R123-free medium. Then, we measured the drug in the medium by spectrofluorometry at different times. Before performing the experiments, we did dose concentration measurements of the R123 inside the trophozoites or dissolved in the TYI-S-33 medium without serum. Curves obtained from these experiments were used as standards. Data obtained revealed that fluorescence emitted by the drug inside the trophozoites is quenched by intracellular components, as described for mammalian cells.[1] Due to this effect, registers were always lower inside the trophozoites than in the culture medium. However, data obtained from confocal microscopy assays showed that after 30 min of incubation with R123, the trophozoites of both clones appeared loaded with a similar amount of R123 (Fig. 8A, B). The relative fluorescence measurements obtained by spectrofluorometry showed that the trophozoites of clone A, after 270 min, maintained the intracellular concentration of the drug, whereas in the trophozoites of clone C2(225) it diminished (data not shown). In contrast, the R123 concentration in the medium of the drug-resistant trophozoites was higher than in clone A during the whole experiment (Fig. 8C).

Using Eq. 1, we calculated the constant rates of R123 efflux.

FIG. 4. Immunolocation of EhPgp proteins in drug-sensitive and -resistant trophozoites by confocal microscopy. Permeabilized trophozoites were first incubated with the anti-EhPgp384 polyclonal antibodies and then with FITC-labeled secondary antibodies (green). Nuclei were counterstained with propidium iodide (red). (**A**) Clone A. (**B**) Clone C2. (**C**) Clone C2(225). Arrows, Protuberances. (**D**) Negative control, in which the first antibody was omitted; bars as indicated in each panel.

FIG. 7. Subcellular distribution of R123 in drug-resistant trophozoites by confocal microscopy. Trophozoites of clone C2(225) were incubated with 5 μg/ml of R123 (green) for 30 min and then permeabilized and incubated with the anti-EhPgp384 antibodies and TRITC-labeled goat anti-rabbit IgGs (red). (**A**) Merging images of trophozoites. Arrows, Cellular protuberances. (**B**) Magnification of a vesicular structure. (**C**) Internal control in which R123 and anti-EhPgp384 antibodies were omitted. Bar, as indicated in **A**.

FIG. 8. R123 efflux kinetics of drug-sensitive and -resistant trophozoites. (**A** and **B**) Fluorescence displayed by trophozoites of clones A and C2(225), respectively, incubated with 1 μg R123/ml medium (green) for 30 min. (**C**) R123 efflux kinetics displayed by clone A (▲) and C2(225) (●) trophozoites. (**D**) Inhibitory effect of verapamil on R123 efflux after 270 min of incubation without verapamil (□), or with verapamil (■). Bars, Mean ± standard deviation.

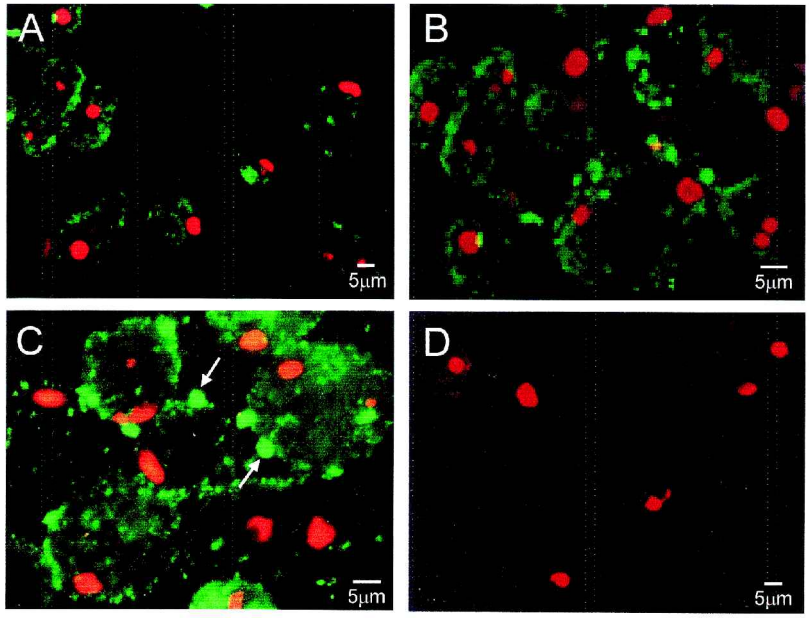

FIG. 4.

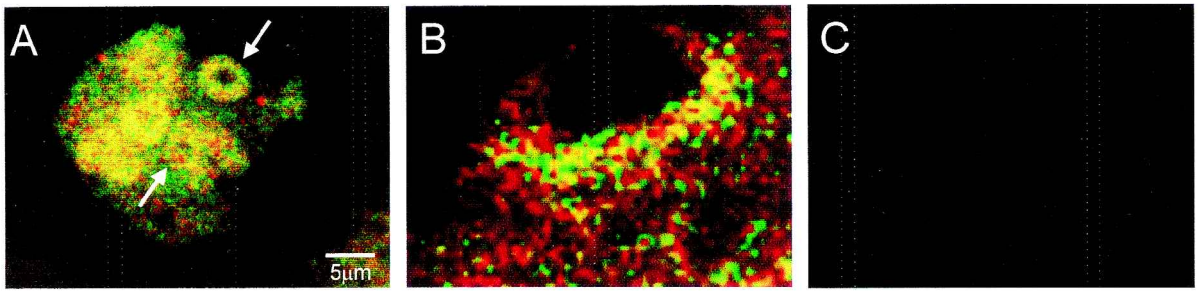

FIG. 7.

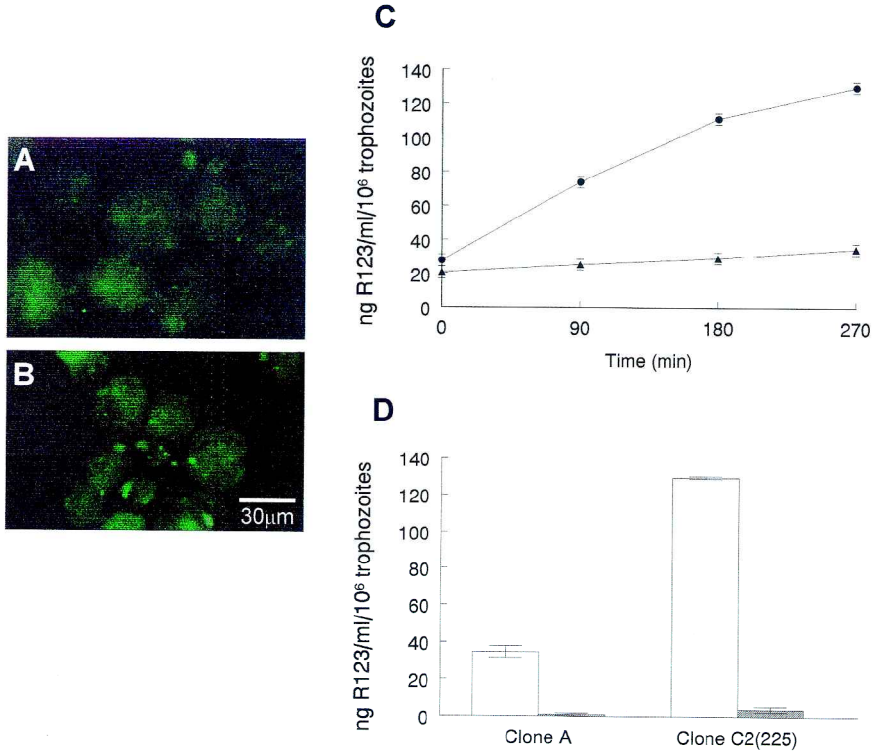

FIG. 8.

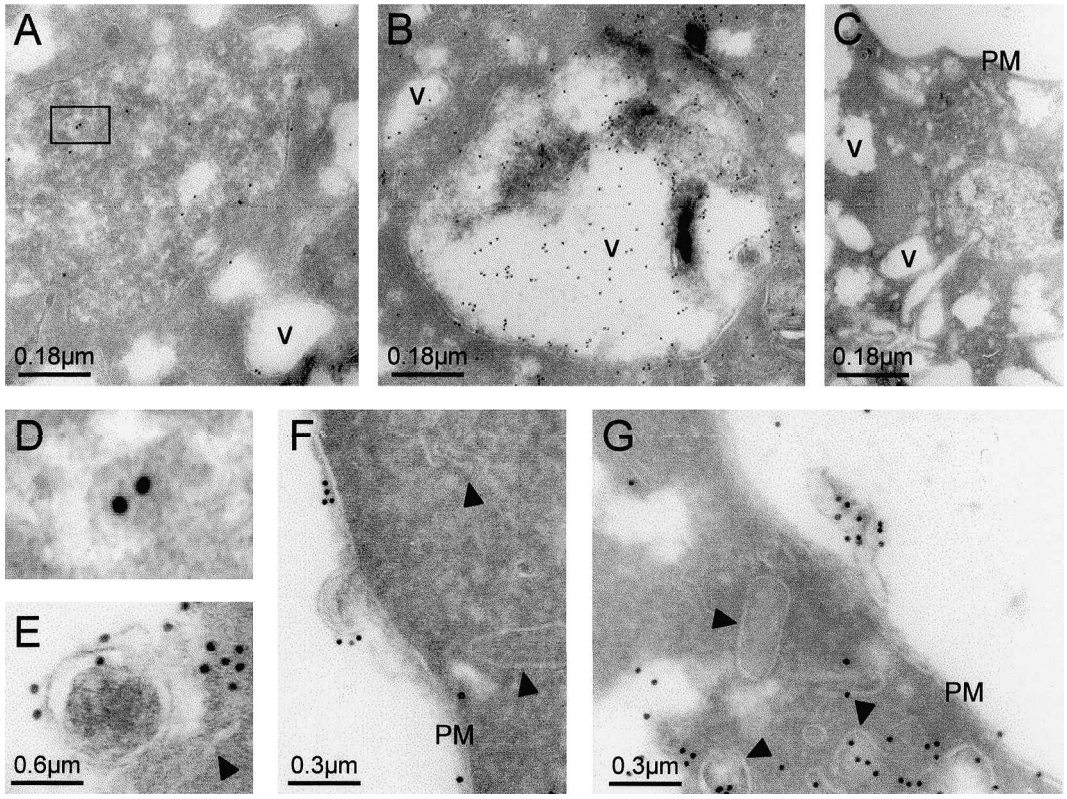

FIG. 5. Subcellular location of EhPgp proteins in drug-sensitive and -resistant trophozoites by TEM. Sections were incubated with the anti-EhPgp384 antibodies and 15-nm gold particle-labeled goat anti-rabbit IgGs. (**A**) Clone A. (**B**) Clone C2(225). (**C**) Negative control, cryosections without the first antibody. (**D**) Magnification of the square in **A**. (**E**), (**F**), and (**G**) Vesicular structures in which EhPgps are located. Arrowheads, Vesicular network; PM, plasma membrane; V, vesicles; bars, as indicated in panels.

For resistant trophozoites, it was 0.4 ng of R123/ml per min per 10^6 trophozoites, whereas in the sensitive ones was 0.1 ng of R123/ml per min per 10^6 trophozoites. The efflux displayed by the clone C2(225) correlated with the expression level of EhPgps detected by Western blot and the microscopy assays (Figs. 3–6).

In the presence of verapamil, constant rates during the entire experiment diminished to 0.012 ng of R123/ml per min per 10^6 trophozoites in clone A and to 0.21 ng of R123/ml per min per 10^6 trophozoites in clone C2(225), confirming that verapamil inhibits drug efflux. Figure 8D shows that after 270 min the amount of drug was very low in the medium of the trophozoites of both clones incubated with verapamil. At the end of all the experiments performed, cell number was maintained and the viability of the cells was 98%.

DISCUSSION

In mammalian cells, Pgps are located at the plasma membrane and they transport drugs out of the cells, avoiding accumulation in toxic concentrations.[16] In *E. histolytica,* EhPgp1 and EhPgp5 proteins seem to be responsible for the MDR phenotype.[31] Recently, we have shown that the EhPgp5 protein,

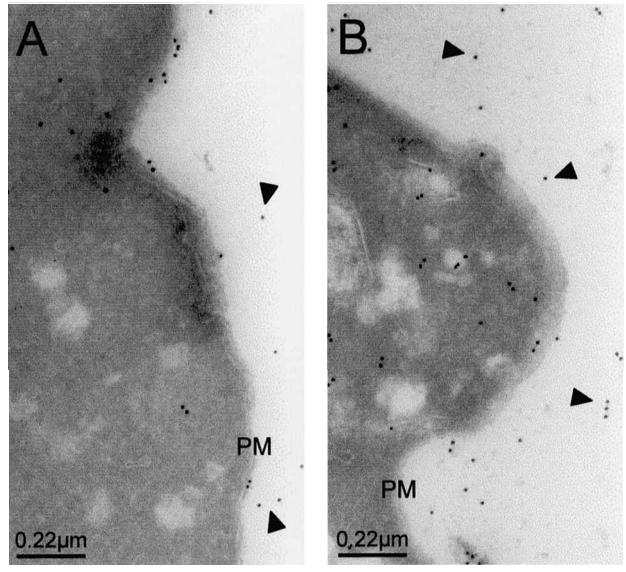

FIG. 6. Extracellular location of EhPgp proteins by TEM. Cells were treated as in Fig. 5. (**A**) Clone A. (**B**) Clone C2(225). Arrowheads, EhPgps; PM, plasma membrane; bars, as indicated in panels.

expressed in *X. laevis* oocytes, could function as a chloride channel or a chloride channel regulator.[10] However, no other studies have been done regarding the drug transport function of the EhPgps.

Here, we present data suggesting that the 147-kDa protein recognized by the anti-EhPgp384 antibodies is encoded at least for the *EhPgp1* and the *EhPgp5* genes, as was shown by the Western blot and RT-PCR assays (Fig. 2D, E). EhPgps have a lower molecular weight than mammalian Pgps. However, they are in the range of the estimated molecular weight previously reported for other Pgps (130–200 kDa).[13,20] According to the expression patterns of the *EhPgp1* and *EhPgp5* genes, EhPgp proteins are differentially expressed in drug-sensitive and -resistant trophozoites (Fig. 3), and their amount in both clones is in concordance with the *EhPgp* mRNA expression level previously reported.[12] Our findings evidenced a remarkable consistence in all experiments for quantitative and qualitative differences found between EhPgps of clones A and C2(225). There exist three to four times more EhPgps in clone C2(225) than in clone A and this produces an emetine-resistance up to 8 μM in clone A and up to 220 μM in clone C2(225).

EhPgps were mainly distributed at the plasma membrane of drug-sensitive and -resistant trophozoites. Additionally, drug-resistant cells presented several fluorescent protuberances, indicating the accumulation of EhPgps, which are probably exported out of the cells. This mechanism may be related to the extrusion of the emetine in which trophozoites were grown.

Interestingly, TEM assays demonstrated that EhPgps were also located in a complex vesicular network that resembles a Golgi-like structure. No typical Golgi apparatus has been found in *E. histolytica.* However, the identification of molecular markers, characteristic of compartments involved in protein trafficking, has provided evidence for the existence of endoplasmic reticulum- and Golgi-like functional compartments in *E. histolytica.*[38] In addition, confocal and TEM studies have also suggested the presence of these structures in this parasite.[18,27] Therefore, it is probable that EhPgps may concentrate, transport, and expel the drug using Golgi-like vesicles. Pgps have also been located in vesicular structures in multidrug-resistant human cancer cells[44] and on the surface of the digestive vacuoles of *Plasmodium falciparum.*[9]

Two action mechanisms for the Pgps pump function have been proposed: (1) Pgps remove drugs directly from the plasma membrane,[35,41] or (2) Pgps pump drugs into subcellular organelles, keeping them from reaching their target sites.[40] Confocal microscopy assays of R123 distribution in resistant trophozoites demonstrated the association of R123 and EhPgps in both plasma membrane protuberances and intracellular vesicles. These observations support the idea that in *E. histolytica* the drugs could be trapped and concentrated in cytoplasmic vesicles, and then transported to the plasma membrane where they are secreted. However, data obtained here do not discard the direct drug extrusion by EhPgps located at the plasma membrane.

Efflux of R123 was faster in clone C2 than in clone A, and in both cases it was proportional to the time course and was measurable only after 30 min of interaction. At shorter times, the efflux was almost null (data not shown). It is possible that the amount and the expression of the different EhPgp members in the cell are responsible for the different drug extrusion velocities observed in trophozoites of clones C2 and A. It is also probable that, in addition to these proteins, other factors may be participating to produce this phenomenon. Further investigations are currently underway to determine the concerted interplay of the mechanisms conferring the MDR phenotype in *E. histolytica* trophozoites.

ACKNOWLEDGMENTS

This work was supported by CONACYT (México) and by an international research scholar award from the Howard Hughes Medical Institute (USA) given to E.O. We express our gratitude to Alfredo Padilla for his help in the artwork.

REFERENCES

1. **Altenberg, G., C.G. Vanoye, J.K. Horton, and L. Reuss.** 1994. Unidirectional fluxes of rhodamine 123 in multidrug-resistant cells: evidence against direct drug extrusion from the plasma membrane. Proc. Natl. Acad. Sci. USA **91:**4654–4657.
2. **Ausubel, F.M., R. Brent, R.E. Kingston, D. Moore, J.G. Seidman, J.A. Smith, and K. Struhl.** 1994. Current protocols in molecular biology. John Wiley & Sons, New York.
3. **Ayala, P., J. Samuelson, D. Wirth, and E. Orozco.** 1990. *Entamoeba histolytica*: physiology of multidrug resistance. Exp. Parasitol. **71:**169–175.
4. **Biagi, F.** 1981. Amebiasis. Antibiot. Chemother. **30:**20–27.
5. **Burchard, G.D., and D. Mirelman.** 1988. *Entamoeba histolytica:* virulence potential and sensitivity to metronidazole and emetine of four isolates possessing nonpathogenic zymodemes. Exp. Parasitol. **66:**231–242.
6. **Canitrot, Y., and D. Lautier.** 1995. Use of rhodamine 123 for the detection of multidrug resistance. Bull. Cancer. **82:**687–697.
7. **Cedeño, J.R., and D.J. Krogstad.** 1983. Susceptibility testing of *Entamoeba histolytica.* J. Infect. Dis. **148:**1090–1096.
8. **Cowman, A.F., and S.R. Karcz.** 1991. The *pfmdr* gene homologues of *Plasmodium falciparum.* Acta Leiden. **60:**121–129.
9. **Cowman, A.F., S.R. Karcz, D. Galatis, and J.G. Culvenor.** 1991. A P-glycoprotein homologue of *Plasmodium falciparum* is localized on the digestive vacuole. J. Cell Biol. **113:**1033–1042.
10. **Delgadillo, D.M., D.G. Pérez, C. Gómez, A. Ponce, F. Paz, C. Bañuelos, L. Mendoza, C. López, and E. Orozco.** 2002. The *Entamoeba histolytica* EhPgp5 (MDR-like) protein induces swelling of the trophozoites and alters chloride dependent currents in *Xenopus laevis* oocytes. Microb. Drug. Resist. **8:**15–26.
11. **Descoteaux, S., P. Ayala, J. Samuelson, and E. Orozco.** 1992. Primary sequences of two P-glycoprotein genes in *Entamoeba histolytica.* Mol. Biochem Parasitol. **54:**201–211.
12. **Descoteaux, S., P. Ayala, J. Samuelson, and E. Orozco.** 1995. Increase in mRNA of multiple *EhPgp* genes encoding P-glycoprotein homologues in emetine-resistant *Entamoeba histolytica* parasites. Gene **164:**179–184.
13. **Di Pietro, A., G. Dayan, G. Conseli, E. Steinfels, T. Krell, D. Trompier, H. Baubichon-Cortay, and J.M. Jault.** 1999. P-glycoprotein-mediated resistance to chemotherapy in cancer cells: using recombinant cytosolic domains to establish structure-function relationships. Braz. J. Med. Biol. Res. **32:**925–939.
14. **Diamond, L.S., R. Harlow, and C. Cunick.** 1978. A new medium for axenic cultivation of *Entamoeba histolytica* and other *Entamoeba.* Trans. R. Soc. Trop. Med. Hyg. **72:**431–432.
15. **DNAStar, Inc.** 1994. March. Madison, Wisconsin.
16. **Endicott, J.A., and V. Ling.** 1989. The biochemistry of P-glyco-

protein mediated multidrug resistance. Annu. Rev. Biochem. **58:**137–171.

17. **Entner, N., L.A. Evans, and C. González.** 1962. Genetics of *Entamoeba histolytica:* differences in drug sensitivity between Laredo and other strains of *Entamoeba histolytica*. J. Protozool. **9:**466–468.
18. **Gosh, S.K., J. Field, M. Frisardi, B. Rosenthal, Z. Mai, R. Rogers, and J. Samuelson.** 1999. Chitinase secretion by encysting *Entamoeba invadens* and transfected *Entamoeba histolytica*: localization of secretory vesicles, endoplasmic reticulum and Golgi apparatus. Infect. Immun. **667:**3073–3081.
19. **Gómez, C., D.G. Pérez, E. López-Bayghen, and E. Orozco.** 1998. Transcriptional analysis of the *EhPgp1* promoter of *Entamoeba histolytica* multidrug-resistant mutant. J. Biol. Chem. **273:**7277–7284.
20. **Grogl, M., R.K. Martin, A.M.J. Oduola, W.K. Milhous, and D.E. Kyle.** 1991. Characteristics of multidrug resistance in *Plasmodium* and *Leishmania*: detection of P-glycoprotein like components. Am. J. Trop. Med. Hyg. **45:**98–111.
21. **Hamann, L., R. Nickel, and E. Tannich.** 1995. Transfection and continuous expression of heterologous genes in the protozoan parasite *Entamoeba histolytica*. Proc. Natl. Acad. Sci. USA **92:**8975–8978.
22. **Hanna, R.M., M.H. Dahniya, S.S. Badr, and A. El-Betagy.** 2000. Percutaneous catheter drainage in drug-resistant amoebic liver abscess. Trop. Med. Int. Health. **5:**578–581.
23. **Hartfield, C., A. McDowall, B. Loveland, and K. Fischer Lindahl.** 1991. Cellular location of thymus-leukemia (TL) antigen as shown by immuno-cryoultramicrotomy. J. Electron Microsc. Tech. **18:**148–156.
24. **Johnson, P.J., B.L. Schuck, and M.G. Delgadillo.** 1994. Analysis of a single-domain P-glycoprotein-like gene in the early-diverging protist *Trichomonas vaginalis*. Mol. Biochem. Parasitol. **66:**127–137.
25. **Johnstone, J.W., A.A. Ruefli, and M. Smyth.** 2000. Multiple physiological functions for multidrug transporter P-glycoprotein? Trends Biochem. Sci. **25:**1–6.
26. **Juliano, R.L., and V.A. Ling.** 1976. A surface glycoprotein modulating drug permeability in Chinese hamster ovary cell mutants. Biochem. Biophys. Acta **455:**152–162.
27. **Mazzuco, A., M. Benchimol, and W. De Souza.** 1997. Endoplasmic reticulum and Golgi-like elements in *Entamoeba*. Micron **28:**241–247.
28. **Norris, S.M., and J.I. Ravdin.** 1990. The pharmacology of antiamebic drugs. *In* J.I. Ravdin (ed.) Amebiasis human infection by *Entamoeba histolytica*. John Wiley & Sons, Inc., New York, pp. 734–755.
29. **Orozco, E., F. De la Cruz Hernández, and M. Rodríguez.** 1985. Isolation and characterization of *Entamoeba histolytica* mutants resistant to emetine. Mol. Biochem. Parasitol. **15:**49–59.
30. **Orozco, E., D.G. Pérez, M.C. Gómez, and P. Ayala.** 1995. Multidrug resistance in *Entamoeba histolytica*. Parasitol. Today **11:**473–475.
31. **Orozco, E., C. Gómez, and D.G. Pérez.** 1999. Physiology and molecular genetics of multidrug resistance in *Entamoeba histolytica*. Drug Resist. Up. **2:**188–197.
32. **Ouellette, M., and B. Papadopoulou.** 1993. Mechanisms of drug resistance in *Leishmania*. Parasitol. Today. **9:**150–153.
33. **Pérez, D.G., C. Gómez, E. López-Bayghen, E. Tannich, and E. Orozco.** 1998. Transcriptional analysis of the *EhPgp5* promoter of *Entamoeba histolytica* multidrug-resistant mutant. J. Biol. Chem. **273:**7285–7292.
34. **Prabhu, R., R. Sehgal, A. Chakraborti, N. Malla, N.K. Ganguly, and R.C. Mahajan.** 2000. Isolation of emetine resistant clones of *Entamoeba histolytica* by petri dish agar method. Indian J. Med. Res. **111:**11–13.
35. **Raviv, Y., H.B. Pollard, E.P. Bruggemann, I. Pastan, and M.M. Gottesman.** 1990. Photosensitized labeling of a functional multidrug transporter in living drug-resistant tumor cells. J. Biol. Chem. **265:**3975–3980.
36. **Samuelson, J., P. Ayala, E. Orozco, and D. Wirth.** 1990. Emetine-resistant mutants of *Entamoeba histolytica* overexpress mRNAs for multidrug resistance. Mol. Biochem. Parasitol. **38:**281–290.
37. **Samuelson, J., A. Burke, and J. Courval.** 1992. Susceptibility of an emetine-resistant mutant of *Entamoeba histolytica* to multiple drugs and to channel blockers. J. Antimicrob. Chemother. **36:**2392–2397.
38. **Sánchez-López, R., S. Gama-Castro, M.A. Ramos, E. Merino, P.M. Lizardi, and A. Alagón.** 1998. Cloning and expression of the *Entamoeba histolytica* ERD2 gene. Mol. Biochem. Parasitol. **92:**355–359.
39. **Sanger, F., S. Nicklen, and A.R. Coulson.** 1977. DNA sequencing with chain-terminating inhibitors. Proc. Natl. Acad. Sci. USA **74:**5463–5467.
40. **Schuurhuis, G.J., H.J. Broxterman, A. Cervantes, T.H. van Heijningen, J.H. de Lange, J.P. Baak, H.M. Pinedo, and J. Lankelma.** 1989. Quantitative determination of factors contributing to doxorubicin resistance in multidrug-resistant cells. J. Natl. Cancer Inst. **81:**1887–1892.
41. **Sharom, F.J.** 1997. The P-glycoprotein efflux pump: how does it transport drugs? J. Membrane Biol. **160:**161–175.
42. **Ullman, B.** 1995. Multidrug resistance and P-glycoproteins in parasitic protozoa. J. Bioenerg. Biomemb. **27:**77–84.
43. **Upcroft, J.A., and P. Upcroft.** 1993. Drug resistance in *Giardia*. Parasitol. Today **9:**187–190.
44. **Willingham, M.C., N.D. Richert, M.M. Cornewell, T. Tsuruo, H. Hamada, M.M. Gottesman, and I. Pastan.** 1987. Immunocytochemical localization of P170 at the plasma membrane of multidrug-resistant human cells. J. Histochem. Cytochem. **35:** 1451–1456.
45. **World Health Organization.** 1997. Weekly Epidemiological Record. **72:**97–100.

Address reprint requests to:
Dr. Guillermo Pérez
Program of Molecular Biomedicine
ENMyH-IPN, Guillermo Massieu Helguera #239
Fracc. "La Escalera"
Ticomán. CP 07320, México, D.F.

E-mail: ishiwaramx@yahoo.com.mx